REPORT DOCUMENTATION PAGE

Form Approved

OMB No. 0704-0188

1. REPORT DATE *(DD-MM-YYYY)*	2. REPORT TYPE	3. DATES COVERED *(From - To)*
21-05-2014	Final	04/16/2013 – 04/15/2014

4. TITLE AND SUBTITLE

Metal Nanoshells for Plasmonically Enhanced Solar-to-Fuel Photocatalytic Conversion

5a. CONTRACT NUMBER
FA2386-13-1-4032

5b. GRANT NUMBER
Grant AOARD-134004

5c. PROGRAM ELEMENT NUMBER
61102F

6. AUTHOR(S)

Prof. Tai-Chou Lee

5d. PROJECT NUMBER

5e. TASK NUMBER

5f. WORK UNIT NUMBER

7. PERFORMING ORGANIZATION NAME(S) AND ADDRESS(ES)

National Central University
No.300, Jhongda Rd
Jhongli City, Taoyuan 320
Taiwan

8. PERFORMING ORGANIZATION REPORT NUMBER

N/A

9. SPONSORING/MONITORING AGENCY NAME(S) AND ADDRESS(ES)

AOARD
UNIT 45002
APO AP 96338-5002

10. SPONSOR/MONITOR'S ACRONYM(S)

AFRL/AFOSR/IOA(AOARD)

11. SPONSOR/MONITOR'S REPORT NUMBER(S)

AOARD-134032

12. DISTRIBUTION/AVAILABILITY STATEMENT

Distribution A: Approved for public release. Distribution is unlimited

13. SUPPLEMENTARY NOTES

14. ABSTRACT

In this study, first, we prepared ternary component semiconductor powders of ZnmIn2S3+m (ZIS) by using microwave-assisted hydrothermal method. Microwave-assisted hydrothermal process is a facile way to produce nanomaterials at a shorter reaction time with less secondary impurities while changing the amount of zinc in a series of solid solutions. With little adjustment of the ratios of [Zn]/[In], the hydrogen production rate of the photocatalysts, particle sizes, and band gap are significantly different. In the following experiments, the core-shell of nanoshell@SiO2, as well as the nanostructure of photocatalyst, were further investigated. Solar energy in the visible-light range is expected to be absorbed by the photocatalyst first without any interference from the metal nanoshells. The presence of metal nanoshells as the core can absorb the solar energy in the IR and visible-light region ranging from 500 nm to 900 nm. Our data showed that the plasmonic-enhanced photocatalytic activity was a function of the absorption of Au nanoshells. At the absorption wavelength of 500 nm of the Au nanoshells, the enhancement of hydrogen production was probably due to the plasmonic effect. As opposed to the absorption wavelength at 900 nm, the enhancement was due to thermal effect. Furthermore, the nanoshell absorbing at 700 nm has the highest hydrogen production rate which may be due to both the plasmonic and thermal effect. Thickness of the silica layer also influenced hydrogen evolution. Steady-state photoluminescence measurement was used to investigate the electron-hole recombination mechanism. Results demonstrated that efficient electron-hole charge separation can be achieved when Au nanoshells were incorporated. Finally, the core-shell with various [Zn]/[In] compositions was used to identify the interaction between the Au nanoshell and the photocatalyst.

15. SUBJECT TERMS

Metal Nanoshells, Metal Nanoshells, Photocatalysts, Hydrogen Generation

16. SECURITY CLASSIFICATION OF:			17. LIMITATION OF ABSTRACT	18. NUMBER OF PAGES	19a. NAME OF RESPONSIBLE PERSON
a. REPORT	b. ABSTRACT	c. THIS PAGE			Jermont Chen, Lt Col, USAF, Ph.D.
U	U	U	UU	11	19b. TELEPHONE NUMBER *(Include area code)* +81-3-5410-4409

Final Report for AOARD Grant FA2386-13-1-4032

"**Metal Nanoshells for Plasmonically Enhanced Solar-to-Fuel Photocatalytic Conversion**"

Date 05/09/2014

Name of Principal Investigators: Tai-Chou Lee

- e-mail address : taichoulee@ncu.edu.tw
- Institution : Department of Chemical and Materials Engineering, National Central University
- Mailing Address : 300 Chung Ta Road, Chung-Li 320 Taiwan
- Phone : +886-3-4227151-34211
- Fax : +886-3-4252296

Period of Performance: 04/16/2013 – 04/15/2014

Abstract

In this study, first, we prepared ternary component semiconductor powders of $Zn_mIn_2S_{3+m}$ (ZIS) by using microwave-assisted hydrothermal method. Microwave-assisted hydrothermal process is a facile way to produce nanomaterials at a shorter reaction time with less secondary impurities while changing the amount of zinc in a series of solid solutions. With little adjustment of the ratios of [Zn]/[In], the hydrogen production rate of the photocatalysts, particle sizes, and band gap are significantly different. In the following experiments, the core-shell of nanoshell@SiO_2, as well as the nanostructure of photocatalyst, were further investigated. Solar energy in the visible-light range is expected to be absorbed by the photocatalyst first without any interference from the metal nanoshells. The presence of metal nanoshells as the core can absorb the solar energy in the IR and visible-light region ranging from 500 nm to 900 nm. Our data showed that the plasmonic-enhanced photocatalytic activity was a function of the absorption of Au nanoshells. At the absorption wavelength of 500 nm of the Au nanoshells, the enhancement of hydrogen production was probably due to the plasmonic effect. As opposed to the absorption wavelength at 900 nm, the enhancement was due to thermal effect. Furthermore, the nanoshell absorbing at 700 nm has the highest hydrogen production rate which may be due to both the plasmonic and thermal effect. Thickness of the silica layer also influenced hydrogen evolution. Steady-state photoluminescence measurement was used to investigate the electron-hole recombination mechanism. Results demonstrated that efficient electron-hole charge separation can be achieved when Au nanoshells were incorporated. Finally, the core-shell with various [Zn]/[In] compositions was used to identify the interaction between the Au nanoshell and the photocatalyst.

Introduction

Of all known renewable energy sources, solar energy stands as the most abundant and readily accessible. Consider, for example, that the amount of solar energy striking the earth every 40 minutes is approximately equal to the amount of energy consumed globally on an annual basis.[1] From this perspective, the United States is fortunate to have vast tracts of land that are suitable for constructing solar power plants; in fact, in the desert Southwest alone there are an estimated 250,000 square miles of suitable land receiving more than 4,500 quadrillion British thermal units (Btu) of solar radiation per year.[1] Converting only 2.5% of that radiation into electricity would equal the total national energy consumption during all of 2006.[1]

The abundance and availability of solar energy has sparked the exploration of a wide variety of solar conversion technologies, including those based on photovoltaics (direct solar to electric), photothermal (solar to heat), and photosynthesis (solar to fuel). In the latter technology, artificial photosynthesis mimics natural photosynthesis by converting water and/or carbon dioxide into fuels and oxygen using sunlight. Splitting water to produce hydrogen and oxygen is one example, and it is the most promising replacement for fossil fuels without any pollutant[2-4]. The development of visible-light-driven photocatalysts for water splitting is critical. ZnS is a highly active photocatalyst for H_2 evolution under UV light irradiation[5, 6]. Because of its wide band gap, the conduction band level is high enough to reduce water. $(AgIn)_xZn_yS_{2x+y}$ solid solution, derived from ZnS is a narrower band gap semiconductor. The absorption of the solid solutions can be tuned from UV light to visible light by adjusting $ZnS/AgInS_2$ ratio. $AgInZn_7S_9$ with a high efficiency of H_2 production is a typical example (~3.3 L/m^2-h).[7] $AgInZn_7S_9$ solid solution with 2.35 eV band gap absorbs the wavelength below 600 nm[8]. For wavelength longer than 600 nm, the light cannot be utilized effectively. This fact has motivated us to search for materials or composite materials that can utilize as much solar energy as possible.

Metal-metal nanoshells (Ag@Au) can absorb the light at different wavelength[9] by altering the thickness of nanoshell (Au). The nanoparticles having an absorption edge in the IR range (>700 nm) can convert the solar energy to heat. According to reaction kinetics, the water splitting reaction rate increases with the temperature. In this study, we wish to explore the development of a unique solar-to-fuel conversion system that is based on the core-shell structure incorporated nanoshells and photocatalysts. Owing to the high processing temperature of $ZnS/AgInS_2$ solid solutions, in this report, the Zn-In-S (ZIS) system was employed as the model system to study the plasmonic-enhanced photocatalytic activity due to metal nanoshells.

Results and Discussion

Preparation of $ZnIn_2S_4$ (ZIS) photocatalysts ZIS photocatalysts with different energy band gaps were synthesized by using microwave-assisted hydrothermal method, carried out in T.-C. Lee's group. An aqueous solution of $In(NO_3)_3 \cdot xH_2O$ (Alfa Aesar; 99.99 %), $Zn(NO_3)_2 \cdot 6H_2O$ (J.T. Baker; 100 %), and thioacetamide (TAA, Sigma Aldrich; 99 %) was used as the precursor solutions. They were prepared in a 50 mL round bottomed flask and mixed well. Prescribed molar ratios in the precursor solutions are listed in Table 1. After 10 min of microwave-assisted hydrothermal reaction at 120 °C, the precipitates were collected and rinsed thoroughly with deionized (DI) water several times. They were then dried at in a 80 ℃ oven for 12 h. Pt co-catalyst was loaded onto the ZIS photocatalysts by the photodeposition method in situ by using $H_2PtCl_6 \cdot 6H_2O$ (Uniregion Bio-tech; 99.95 %).

Table 1. Compositions of the precursor solutions.

Sample	Zn	In
A	1	2
B	2	2
C	3	2
D	4	2
E	5	2

According to our previous studies, the energy band gap of this type of metal sulfide material can be tuned by changing the [Zn]/[In] ratio. We measured the absorption of photocatalyst using UV-Vis spectrometer (Figure 1 Left). The onset of absorption edge of Sample A ([Zn]/[In] = 0.5) was around 580 nm and that of sample E was 500 nm, corresponding to energy band gaps of 2.13 and 2.48 eV, respectively. It is evident that by adjusting the level of indium content, the absorption can be adjusted accordingly. In addition, all the samples exhibited absorption in the visible light region.

Photocatalytic reactions were conducted in a home-made glass cell with a quartz side window. The 300 W Xenon lamp was employed to simulated the sun light. The light path was adjusted and focused on a uniform illumination at the quartz window. The photocatalyst powders, loaded with Pt were dispersed in an aqueous solution containing sacrificial reagents (220 mL of 0.25 M K_2SO_3 and 0.35 M Na_2S) with magnetic stirring. They were then reacted under a Xe lamp with an intensity of 100 mW/cm^2. Hydrogen gas was collected by using the water displacement method. Hydrogen production experiment showed that Sample B ([Zn]/[In] = 1) (Figure 1 Right) has the highest photocatalytic activity. Further increase the [Zn]/[In] ratio decreases the photocatalytic activity. Our experimental results indicate that the utilization of solar spectrum was influenced by many factors, giving rise to an optimal composition. Figure 2a is the XRD patterns of the samples with various [Zn]/[In] ratios, from 0.5 (sample A) to 2.5 (sample E). A shift in the XRD peak positions to a higher angle was observed,

which agrees with those found in the literature[8]. Figure 2b-f shows the SEM images of these photocatalysts. It can be observed that particle size appeared smaller on the samples with higher [Zn]/[In] ratio.

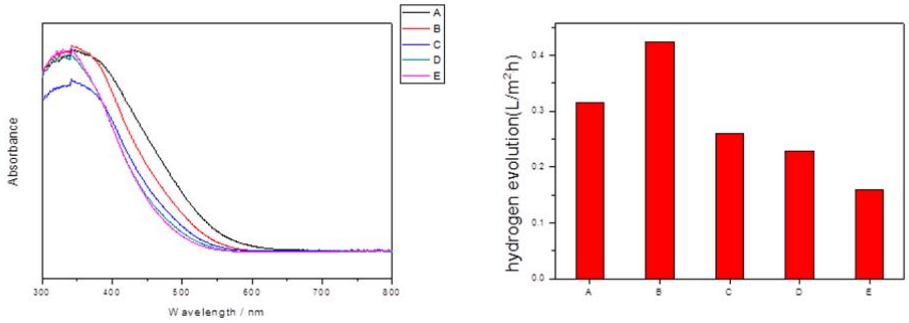

Figure 1: (Left) The UV-Vis absorption patterns for samples with various amount of Zinc. (Right) Hydrogen evolution for samples with various ratio of [Zn]/[In].

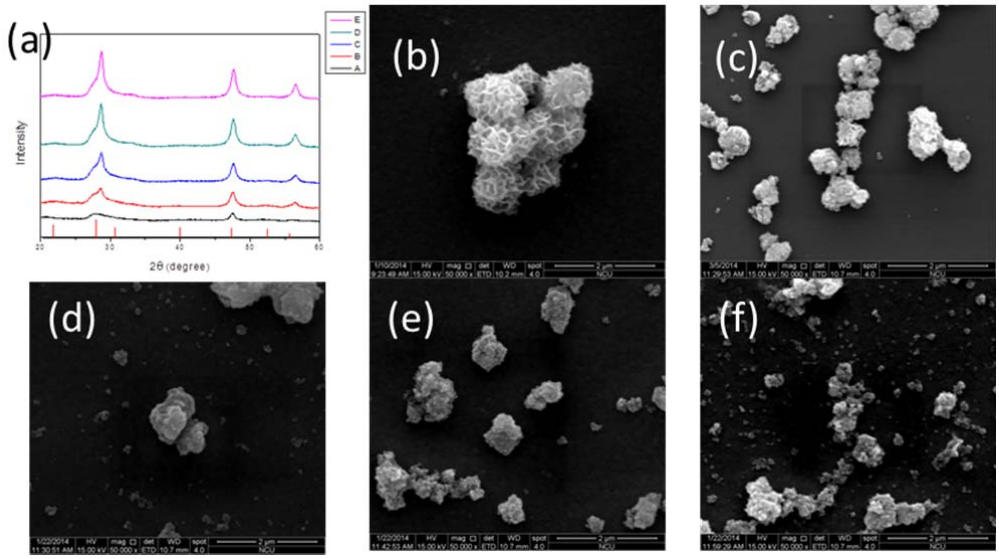

Figure 2: (a) Powder XRD patterns for samples with various ratio of [Zn]/[In], SEM images of samples with [Zn]/[In] = (b)0.5, (c)1.0, (d)1.5, (e)2.0, and (f)2.5.

Synthesis of Au nanoshells (AuNS) Recent research efforts in the T. R. Lee group have focused on the preparation and study of silica-coated plasmonic nanoshells, where the core consists of small hollow silver-gold nanoparticles.[10] In initial collaborative work with the T.-C. Lee group, we prepared uncoated hollow Ag-Au nanoshells possessing a variety of maxima for which the surface plasmon resonance (SPR) peaks were selectively positioned at ~500, 700, and 900 nm in the electromagnetic spectrum. Exploration of this range of absorbances allowed us to develop a better understanding of the interaction of our nanoshells with the photocatalyst under different wavelengths of light. Additionally, we modified the Ag-Au nanoshells and coated them with different thicknesses of silica

shells (~25 and ~50 nm) in order to gain an understanding of the charge-transfer mechanisms of the photocatalytic reactions.

Results from the photocatalysis studies utilizing these initial composite particles led us to conclude that there was a need to improve the homogeneity of the hollow Ag-Au nanoshells -- a problem that was could be traced to the methodology used to prepare the initial Ag nanoparticle core templates. Therefore, we sought to improve the homogeneity of these core particles and that of the corresponding hollow Ag-Au nanoshells derived from them. The success of our new synthetic methodology can be gleaned from Figure 3, where both the Ag nanoparticle cores and the corresponding hollow Ag-Au nanoshells exhibit smoother morphologies and narrower size distributions than those observed in our previous work. Importantly, these nanoshells offer optical properties consistent with the goals of the project, with strong absorption ranging from the visible to the near infrared (see Figure 4).

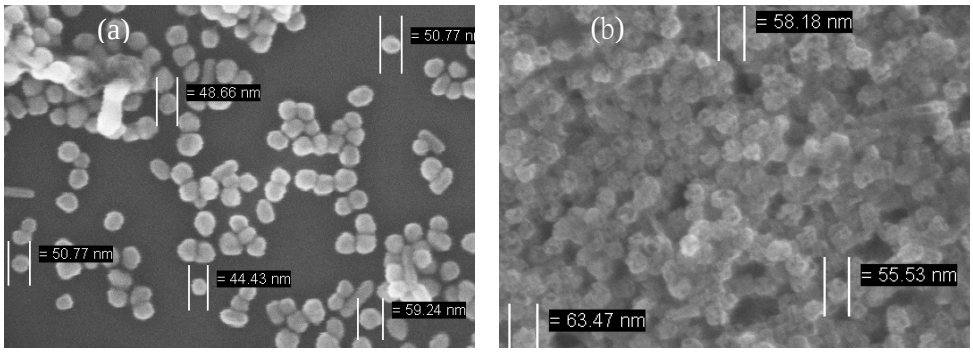

Figure 3: SEM images of (a) silver nanoparticles and (b) uncoated silver-gold nanoshells.

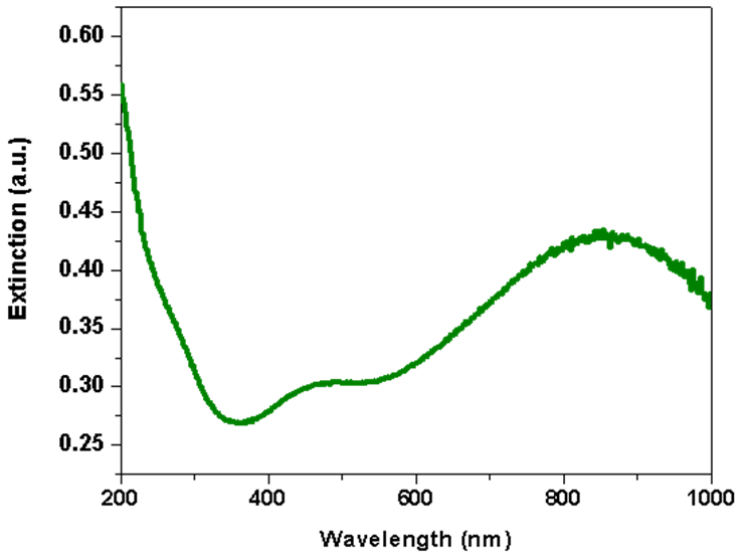

Figure 4: Extinction spectra of homogeneous Ag-Au nanoshells.

To gain control over the interfacial properties of the nanoshells for incorporation into the

photocatalyst architecture and to enhance their stability, we coated the nanoshells with a thin layer of silica. Further, we developed a synthetic route to produce porous silica-coated Ag-Au nanoshells, which allowed us to generate the hollow Ag-Au nanoshells after coating the Ag nanoparticle cores with silica (see Scheme 1). By coating the Ag nanoparticles before forming the Ag-Au hollow nanoshells, the porous silica shell prevents the agglomeration of the composite particles and affords nanoshell structures with enhanced uniformity and more readily tunable optical properties. These advances were recently reported.[11] Figure 5a shows a TEM image of a typical porous silica-coated Ag-Au hollow nanoshell. Importantly, we successfully demonstrated the tunability of the SPR absorption by varying the etching time, as shown in Figure 5b.

Scheme 1. Strategy Used to Synthesize Porous Silica-Coated Hollow Silver-Gold Nanoshells

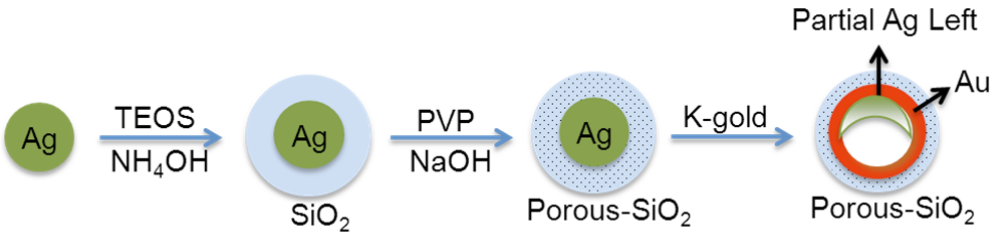

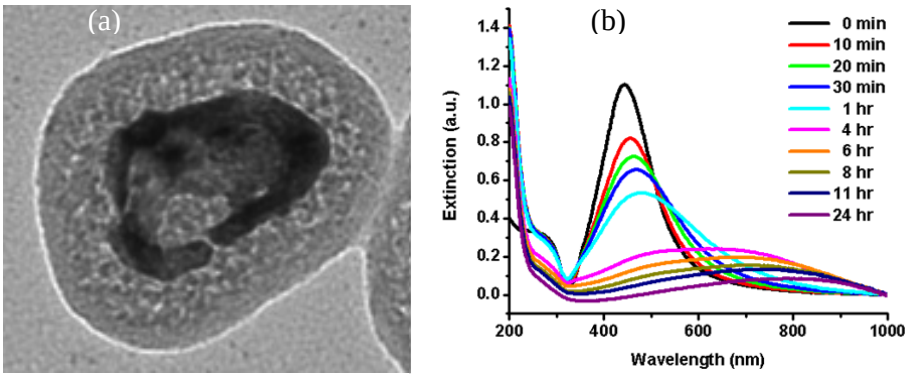

Figure 5: (a) TEM image of a single porous silica-coated hollow Ag-Au nanoshell. (b) Extinction spectra for a series of porous silica-coated hollow Ag-Au nanoshells as a function of the duration of galvanic replacement.

We have also made progress on the synthesis and study of tin oxide-coated hollow Ag-Au nanoshells. Further, we will extend our coating system to include doped tin oxide shells that provide us an opportunity for understanding the role that the shell plays in modulating the photocatalytic reaction by creating an adjustable electron-transfer energy barrier that varies with the nature and amount of the dopant.

AuNS@SiO_2@ZIS composite structure and photocatalytic activity In making the core-shell

structure, the prepared AuNS@SiO_2 were added into the precursor solution and mixed well. After 10 min of microwave-assisted hydrothermal reaction at 120 °C, the precipitates were rinsed thoroughly with deionized (DI) water several times, and they were then dried at 80 °C in an oven for 12 h. The AuNS@SiO_2@ZIS core-shell structures were generated (Figure 6). According to the previous section, the absorption of the AuNS can be adjusted by changing the relative volume of Ag NPs and K-gold solution. The core/shell structure using different nanoshells (NSs) are listed in Table 2. The absorption spectra of various core-shell structures were shown in Figure 7. The absorption spectrum of bare ZIS particles was also plotted as the reference. As demonstrated in this figure, a shoulder at longer wavelength appears in each of the absorption curve. This additional peak match to the position of the absorption of designed AuNS. It is evident that using microwave-assisted hydrothermal synthesis, not only the reaction time is decreased, but the integrity of the AuNS remained intact.

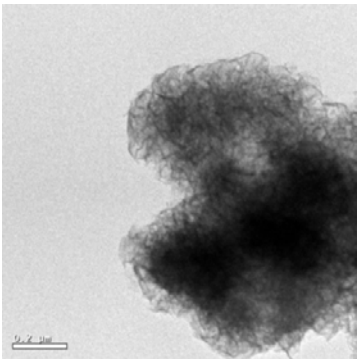

Figure 6: SEM image of core-shell structure.

Table 2. The core/shell structure using different absorption of nanoshells.

Sample	Nanoshell(wavelength)
1	None
2	500nm
3	700nm
4	900nm

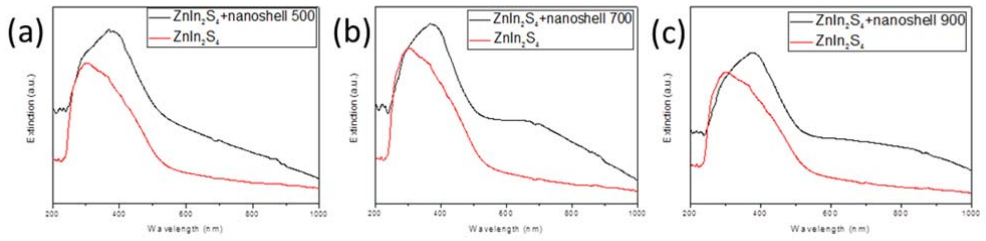

Figure 7: Absorption of core-shell structure, where the absorption of AuNS positioned at (a) 500 nm, (b) 700 nm, and (c) 900 nm.

Hydrogen production experiments were carried out under a 100 W Xe light irradiation with an intensity of 100 mW/cm^2 (

Figure 8). The samples were labeled according to Table 2. In this case, AuNS with no SiO_2 coating, 20-25 nm coating, and 50-60 nm coating were used as the core. It can be clearly seen that the photocatalytic activity of particles with AuNS is higher than that without AuNS. Compared to other AuNS, sample 3 (with absorption at 700 nm) exhibit the highest hydrogen production rate, perhaps due to a better interaction between photocatalyst and AuNS. The hydrogen evolution experiments were carried out at a constant temperature. As a consequence, this enhancement might be attributed to the local surface plasma resonance (LSPR). The SiO_2 thickness has a huge impact on the photocatalytic activity, as demonstrated in

Figure 8 as well. Without SiO_2 buffer layer, no significant enhancement was observed. However, when the SiO_2 thickness is 20-25 nm, the hydrogen production rate is almost doubled. Note that the same weight of the particle was used to generate hydrogen gas. Supposedly, the total weight of ZIS photocatalyst with AuNS core was less than that without AuNS. Therefore, the hydrogen production per weight should be higher. It suggests that the utilization of solar energy is further enhanced. From the experimental data shown about, the plasmonic enhanced hydrogen production is evident.

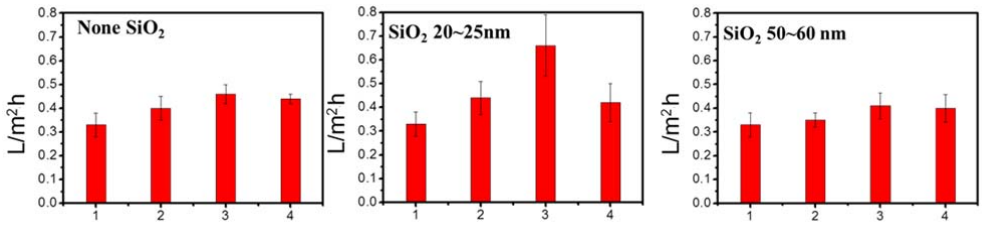

Figure 8: Hydrogen evolution for core/shell with different nanoshells.

To further understand the charge transfer mechanism and pathways, steady-state photoluminescence was employed to investigate the electro-hole recombination for various catalysts. The higher the intensity of PL implies the higher electron-hole recombination rate, which decreases the efficiency of the hydrogen production. Figure 9 shows PL intensities with different thicknesses of SiO_2 between ZIS photocatalyst and AuNS. The thicknesses of SiO_2 layers were 0, 20-25, and 50-60 nm for Figure 9a, b, and c, respectively. It is clearly seen that, first, the PL intensity of the sample without any AuNs was the highest, suggesting high recombination rate. Secondly, the PL intensities of samples with thicker SiO_2 layer remain high. The degree of decrease in PL intensity was less than that of samples with thinner SiO_2 layer. These observations agreed well with hydrogen production data

shown in Figure 8. Without SiO_2 layer, the presence of AuNS can also promote electron-hole separation. Because of the lower work function of Au, it is expected that electrons will transfer to Au from ZIS photocatalysts. It seems the electrons were trapped in the AuNS, hydrogen production rate was suppressed. Unfortunately, PL experiments can not distinguish the differences between samples with difference absorption of AuNS. Detailed investigation using time-resolved PL spectroscopy will be carried out in the future.

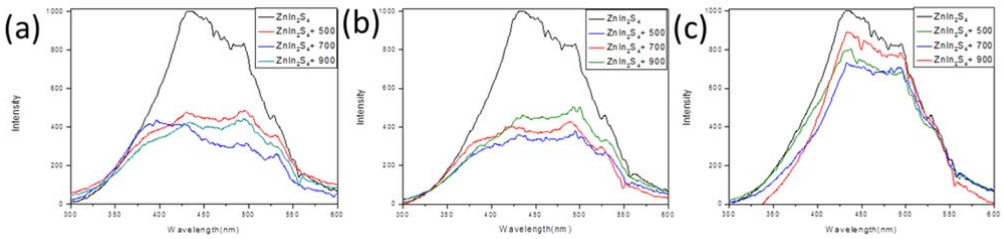

Figure 9: PL spectra for core/shell with different nanoshells. (a) without SiO_2 buffer layer, (b) 20-25 nm SiO_2, and (c) 50-60 nm SiO_2.

Finally, the core-shell with various [Zn]/[Ag] compositions in ZIS was investigated (Figure 10). This figure plots the hydrogen evolution rate as a function of onset of absorption of ZIS particles shown in Figure 1 left. The shorter the absorption edge, the higher [Zn]/[[Ag] ratio. The immobilization of ZIS particles on nanoshells increased the hydrogen production rate, especially for the samples using ZIS particles with onset of absorption larger than 525 nm. Because the LSPR peak appeared at about 500 nm for nanoshells, it was reasonable that the electron-hole pairs generated from ZIS particles with onset of absorption longer than 525 nm were effectively photoexcited with the LSPR induced electric field. It should be noted that the composite particle of AuNS@ZIS (510 nm) exhibited lower photocatalytic activity than that of the corresponding bare ZIS. The exact origin of this phenomenum is not clear..

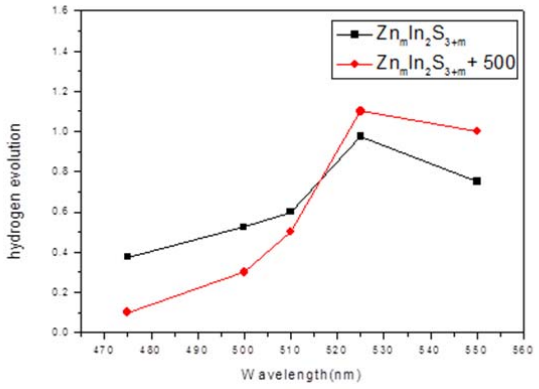

Figure 10: Hydrogen evolution for core/shell with various ratio of [Zn]/[In]. AuNS with 500 nm absorption covered with 20-25 nm SiO_2 was used as the core.

In summary, we first reported the preparation of Zn-In-S (ZIS) ternary component photocatalysts by using microwave-assisted hydrothermal method. The [Zn]/[In] ratio determined the onset of absorption, which leading to different utilizations of the solar spectrum. Samples with various [Zn]/[In] compositions show different photocatalytic activities. Secondly, we fabricate composite structures with Au nanoshells (AuNS) covered by SiO_2 as the core and ZIS photocatalysts as the shell. The efficiency of photcatalysts with AuNS is higher than that of bare photocatalysts due to the plasmonic effect. These experimental findings provide important information for designing next generation composite materials for hydrogen production from water splitting.

Reference

1. K. Zweibel, J. Mason and V. Fthenakis, in *Sci. Am.*, 2008, pp. 64-73.
2. A. Kudo, *Int J Hydrogen Energ*, 2007, **32**, 2673-2678.
3. A. Kudo and M. Sekizawa, *Chemical Communications*, 2000, 1371-1372.
4. D. Chen and J. Ye, *Journal of Physics and Chemistry of Solids*, 2007, **68**, 2317-2320.
5. J.-F. Reber and K. Meier, *Journal of Physical Chemistry*, 1984, **88**, 5903-5913.
6. N. Zeug, J. Bucheler and H. Kisch, *J Am Chem Soc*, 1985, **107**, 1459-1465.
7. I. Tsuji, H. Kato, H. Kobayashi and A. Kudo, *J. Am. Chem. Soc.*, 2004, **126**, 13406-13413.
8. I. Tsuji, H. Kato, H. Kobayashi and A. Kudo, *J Am Chem Soc*, 2004, **126**, 13406-13413.
9. Y. Yang, J. L. Shi, G. Kawamura and M. Nogami, *Scripta Mater*, 2008, **58**, 862-865.
10. V. Vongsavat, B. M. Vittur, W. W. Bryan, J.-H. Kim, T. R. Lee, ACS Appl. Mater. Interfaces **3**, 3616 (2011).
11. C.-H. Li, A. C. Jamison, S. Rittikulsittichai, T-.C. Lee, and T. R. Lee, ACS Photonics, submitted.